Ceramics International 43 (2017) 5450–5456

Contents lists available at ScienceDirect

Ceramics International

journal homepage: www.elsevier.com/locate/ceramint

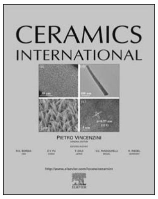

One-pot synthesis of Ag-TiO_2/reduced graphene oxide nanocomposite for high performance of adsorption and photocatalysis

Lixin Zhang[a,*], Changhui Ni[a], Hongfang Jiu[b], Chunmei Xie[a], Jibing Yan[a], Guisheng Qi[c]

[a] *Chemical Engineering And Environment Institute, North University Of China, Taiyuan 030051, People's Republic of China*
[b] *College of Science, North University of China, Taiyuan 030051, People's Republic of China*
[c] *Shanxi Province Key Laboratory of Higee-Oriented Chemical Engineering, Taiyuan 030051, People's Republic of China*

ARTICLE INFO

Keywords:
Graphene
One-pot
Adsorption
Photocatalysis
CO_2

ABSTRACT

The Ag-TiO_2/r-GO nanocomposite was synthesized via a facile one-pot solvothermal method. X-ray diffraction (XRD), Transmission electron microscopy (TEM),High resolution transmission electron microscopy(HRTEM), UV–vis diffuse reflectance spectroscopy (DRS), Fourier transformed infrared spectroscopy (FT-IR), Photoluminescence (PL) and N_2 adsorption-desorption were used for the characterization of prepared samples. The adsorbent and photocatalytic performance of prepared samples were evaluated by remove of Rh B dyes and reduction of CO_2. Both the adsorbent and photocatalytic ability of all the Ag-TiO_2/r-GO samples were much higher than pure hollow TiO_2. The excellent adsorbent capacity can be attributed to the large BET surface area and the enhanced photocatalytic activity can be assigned to the predominant properties of graphene and the localized surface plasmon(LSPR) effect of Ag nanoparticles.

1. Introduction

The past decades had witnessed the fast develop of global economy, which brings lots of environmental problems at the same time. Among them, water pollution and global warming are one of the most rigorous problems , which should be solved by all over the world. The water pollution caused by organic dyes was difficult to remove due to their complex structure and poor ability of biodegradation. These waste water can influence the balance of aquatic plant and influence our human daily life finally [1,2]. The excess of CO_2 led to the rise of sea level, which would submerge some island [3,4]. Because of its green and energy conservation, photocatalytic process has been regard as an ideal method to resolve above problems [5].

Owing to its strong oxidizing power, nontoxicity, high chemical stability, and photostability, TiO_2 has been widely used and studied as photocatalyst [6–8]. However, the band gap of TiO_2 is 3.2 eV, which could only absorb the ultraviolet region of the sunlight. What's more, the high recombination rate of electron-hole pairs, would also greatly limit its practical applications. There are a series of methods to solve these problems such as semiconductor coupling, noble metal and element doping, coupled with carbon materials and so on [9–12].

Graphene, a two-dimensional single-layer graphitic carbon material, has been a potential material for photocatalytic applications because of its unique properties such as high theoretical specific surface area, excellent electrical conductivity, high chemical stability and flexible structure [13,14]. Due to the high electron mobility and extended π-π conjugation structure, graphene is an ideal electron acceptor for nanocomposite during the photocatalytic process, which can suppress the recombination of photoexcited electrons and holes [15,16]. What's more, the high BET surface area of graphene based nanocomposites can provide more active site to absorb reactant molecule [17]. Therefore, graphene based nanocomposites can act as adsorbent and photocatalyst at the same time during the photocatalytic process.

In addition to this, noble metal (Ag or Au) doping is an effectively method to improve photocatalytic performance [18–20]. Ag or Au nanoparticles have the strong ability to absorb photo-generated electron, which can restrain the recombination of electron-hole pair and enhance the photocatalytic activity. Furthermore, the localized surface plasmon effect (LSPR) of Ag or Au nanoparticle can provide the noble metal-TiO_2 nanocomposite with the ability of visible light response [21,22]. There are several research works focusing on Ag-TiO_2/graphene nanocomposite. Vasilaki E et al. prepared Ag-loaded TiO_2/reduced graphene oxide by a two step method. The prepared samples were used to degrade MB dye under visible-light irradiation. The results showed that the photocatalytic activity of TiO_2/Ag(3%)/r-GO(1%) was much higher than pure TiO_2 and TiO_2/Ag nanocomposites [23]. Fan J et al. used $AgNO_3$, P25and graphite oxide as raw materials to prepare Ag-P25-graphene ternary composite. The samples were applied to water splitting. The results revealed that the Ag-P25-graphene ternary composite had a higher ability on hydrogen evolution

---

[*] Corresponding author.

http://dx.doi.org/10.1016/j.ceramint.2017.01.041
Received 18 September 2016; Received in revised form 23 December 2016; Accepted 9 January 2017

than P25 and P25/graphene [24]. Wang M.Q. et al. prepared Ag/r-GO/TiO_2 by a one-pot solvothermal method. The catalysts had high activity both on degrade Rh B and hydrogen generation [25].

However, most research focused on improving the photocatalysis ability of TiO_2 in previous studies. To the best of our knowledge, litter research focused on improving adsorptive and photocatalytic capabilities of TiO_2 at the same time. What's more, the previous literatures focused on the photodegradation of organic pollutant and splitting of water into hydrogen. Few studies investigated the reduction of CO_2 into organics through Ag-TiO_2/r-GO nanocomposite. In this work, Ag-TiO_2/r-GO nanocomposite was synthesized by a one-pot hydrothermal method. The large surface area, excellent properties of r-GO and LSPR of Ag nanoparticles ensure the high performance of adsorption and photocatalysis both on remove of Rh B and reduction of carbon dioxide(CO_2).

2. Experimental

2.1. Materials and reagents

Silver nitrate($AgNO_3$), Potassium bromide(KBr), Sodium dodecyl benzene sulfonate(SDBS), Tetrabutyl titanate(TBOT), Concentrated sulfuric acid(H_2SO_4), Potassium persulfate ($K_2S_2O_8$), Phosphorus pentoxide(P_2O_5), Graphite powder, absolute ethanol. All materials were analytically pure and used without further purification. The deionized water(DI) was used during the experimental process.

2.2. Synthesis of GO

The GO was synthesized through a modified Hummers' method [26]. In detail, 3 g of graphite powder was put into a mixture of 12 mL concentrated H_2SO_4, 2.50 g $K_2S_2O_8$, and 2.50 g P_2O_5. Then the mixture was heated to 80 ℃ and kept stirring for 5 h in a water bath. Then the mixture was diluted with 500 mL water, filtered and washed with deionized water until filtrate to neutral. Then the products were dried under room temperature. The pre-oxidized graphite was added to the 120 mL H_2SO_4 in an ice bath. Thereafter, the product was reoxidized by Hummers and Offeman methods to produce the graphite oxide. Then 15.0 g $KMnO_4$ was slowly added with mechanical stirring. The temperature of the mixture was controlled below 20 ℃ by a ice bath. Then ice bath was removed and the mixture was stirred at 35 ℃ for 2 h. The reaction was terminated by adding 800 mL water and 25 mL 30% H_2O_2 solution. The mixture was filtered and washed with 1:10 HCl aqueous solution to remove metal ions followed by DI water to remove the acid. Finally, the GO was obtained by drying.

2.3. Synthesis of Ag-TiO_2/r-GO

The Ag-TiO_2/r-GO nanocomposite was prepared by a facile one-pot solvothermal method. In a typical synthesis, 40 mg GO was dispersed in 20 mL deionized water under ultrasonic treatment for 2 h. Then, 10 mL 0.01 mol/L $AgNO_3$ aqueous solution was added to the above GO solution and stirred for 12 h. After that, 0.02 g SDBS and 10 mL 0.01 mol/L KBr were slowly added and stirred for another 0.5 h. Subsequently, 20 mL absolute ethanol containing a certain volume of TBOT was dropped into the solution and stirred to get a homogeneous suspension. The homogeneous suspension was sealed into a 100 mL Teflon-lined autoclave and heated at 180 ℃ for 10 h. The resulting samples were washed with deionized water and ethanol several times, and then dried in a vacuum oven under 50 ℃. The obtained powder was dipped in ammonium hydroxide solution for 48 h. The final sample was obtained by washed and dried. The volume of TBOT were 0.5, 1.0, 1.5 and 2 mL, named ATG-1,ATG-2,ATG-3 and ATG-4, respectively. The pure hollow TiO_2 (HT) was prepared by our previous study for blank control [14].

2.4. Characterization

X-ray powder diffraction pattern(XRD) was obtained by a D/MaxRB X-ray diffractometer (Japan) with Cu Kα irradiation source (λ=1.5418 Å) through the 2θ range from 10° to 80. Transmission Electron Microscopy (TEM, JEM-1400 Japan) and High Resolution Transmission Electron Microscopy(HR-TEM, JEOL-2010) were used to test the morphologies of prepared samples. Fourier-transform infrared(FT-IR) spectra with KBr powder-pressed pellets were characterized by Nicoletis 10 (KBrdisk)(China). N_2 adsorption-desorption were carried out by USA Micromeritic ASAP 2020 nitrogen adsorption apparatus. The optical properties of the samples were characterized by a UV-2600 ultraviolet/visible diffuse reflectance spectrophotometer (DRS), during which $BaSO_4$ was employed as the internal reflectance standard. The photoluminescence spectra (PL) were recorded with a Hitachi F-2700 fluorescence spectrophotometer. The concentration of Rh B dyes was obtained by UV-2300 UV–vis(China).

2.5. Adsorption and photodegradation experiment

The adsorbent ability and photodegradable activity of prepared samples were evaluated by remove of RhB. In a typical process, 30 mg catalyst and 50 mL 10 mg/L RhB solution were placed in a quartz vessel, the suspension was stirred at dark to evaluated the adsorbent ability. A 300 W Xe lamp with a 420 nm optical filter was turned on when getting the adsorption- desorption equilibrium. Approximately 3 mL of the suspension was taken out every 10 min and centrifuged to remove the catalysts. The photodegradable activity was observed by measuring the absorbance of the supernatant by ultraviolet spectrophotometer.

2.6. Photocatalytic reduction of CO_2

The CO_2 reduction reaction was tested by a quartz glass tube with a volume of 60 mL containing 50 mg catalyst in 50 mL 1.0 mol/L NaOH solution. Then bubbling the CO_2 gas for 0.5 h persistently under darkness. Turned on the 300 W Xe lamp with a 420 nm optical filter after the CO_2 get an equilibrium. During the photocatalytic process, approximately 4 mL liquid product was taken out per 1 h and centrifuged to remove the catalysts. The concentration of main liquid products(Methanol and Ethanol) was analyzed by a gas chromatograph. (GC-920) equipped with a flame ionization detector and capillary column. The experiments of No photocatalyst, no visible light irradiation and replacing CO_2 by N_2 were done for contrast.

3. Results and discussion

3.1. Characterization of ATG samples

The crystalline phases of Ag-TiO_2/r-GO and GO were examined by XRD patterns(Fig. 1). According to the XRD Pattern, GO shows a diffraction peak(002) at a 2θ value of 9.6°, which indicated that GO was successfully synthesized by graphite powder through modified Hummers methods [27]. It is clear to see that the diffraction peak of Ag-TiO_2/r-GO located at 2θ=25.3°, 38.0°, 48.0°, 53.9°, 55.1°, 62.9°, 69.0°, 70.1° and 75.4°, which can be assigned to the (101), (004), (200), (105), (211), (204), (116), (220), and (215) crystal planes of anatase TiO_2 respectively (JCPDS card21-1272) [28]. Because the amount of Ag is low and AgBr was dissolved by ammonium hydroxide, no diffraction peaks of Ag or AgBr were observed. Moreover, the XRD peak of GO at 2θ=9.6° disappeared after solvothermal reaction, suggesting that most GO has been reduced. In addition, no typical diffraction peaks of r-GO were observed in the Ag-TiO_2/r-GO pattern because the main r-GO diffraction peak at 25.0° overlapped with the stronger peak of anatase TiO_2 at 25.3° [29]. The XRD patterns of all ATG samples were shown in Fig. S1. As shown, the diffraction peaks of